

Temperature Dependence of the Rate Constant and Product Distribution of the Reaction of CH₃ Radicals with O(³P) Atoms

Christopher Fockenberg* and Jack M. Preses†

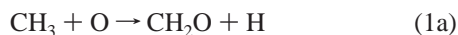
Chemistry Department 555A, Brookhaven National Laboratory, P.O. Box 5000, Upton, New York 11973-5000

Received: November 14, 2001; In Final Form: January 16, 2002

The kinetics and product distribution for the reaction of methyl radicals, CH₃, with ground-state, O(³P) oxygen atoms, have been investigated at temperatures up to 925 K and at constant bath gas (He) concentrations of about $3.2 \times 10^{16} \text{ cm}^{-3}$. With a photoionization/time-of-flight mass spectrometer (TOFMS) as an analytical tool, precursor species, reactants, and products were observed simultaneously. The radicals were produced by an excimer laser pulse ($\lambda = 193 \text{ nm}$), in the cophotolysis of acetone, CH₃C(O)CH₃ and sulfur dioxide, SO₂. In addition to the dominant product, formaldehyde (CH₂O), carbon monoxide (CO) was detected as the only other main product. The yields for both products were found to be independent of temperature with values of $\Phi_{\text{CH}_3+\text{O}}(\text{CH}_2\text{O}) = 0.84 \pm 0.12 (2\sigma)$ and $\Phi_{\text{CH}_3+\text{O}}(\text{CO}) = 0.15 \pm 0.06 (2\sigma)$. However, the overall rate constant for this reaction shows a slight increase with temperature with $k_{\text{CH}_3+\text{O}} = (2.4 \pm 0.3) \times 10^{-10} \exp(-202 \pm 60 \text{ K}/T) \text{ cm}^3 \text{ molecule}^{-1} \text{ s}^{-1}$ between $T = 354$ and 925 K at $[\text{He}] = 3.2 \times 10^{16} \text{ cm}^{-3}$. In an additional experiment the rate constant for the reaction of deuterated methyl radicals, CD₃, with oxygen atoms at 308 K in 3 Torr of He was determined to be $k_{\text{CD}_3+\text{O}} = (1.3 \pm 0.8) \times 10^{-10} \text{ cm}^3 \text{ molecule}^{-1} \text{ s}^{-1}$. Using tunable diode laser absorption spectroscopy (TDLAS) the product yield of C¹⁸O from the reaction CD₃ + ¹⁸O(³P) was measured at room temperature in 5 Torr of Ar indicating an H/D-isotope effect lowering the yield to $\Phi_{\text{CD}_3+\text{O}}(\text{C}^{18}\text{O}) = 0.12 \pm 0.01 (2\sigma)$.

Introduction

The temperature dependence of the rate constant and product distribution of the reaction of methyl radicals with oxygen atoms has been measured, continuing an earlier study in our laboratory, in which the kinetics and product distribution of this reaction had been determined at room temperature. Formaldehyde and carbon monoxide were identified as main products with yields of 0.84 ± 0.15 and 0.17 ± 0.11^1 and 0.18 ± 0.04^2



Recently, Marcy et al.³ investigated the isotope effect on the product yield for the reactions of CH₃ + O and CD₃ + O by observing IR emission from the CO produced in either reaction. Exchanging H with D atoms dropped the yield of channel (1b) by about 30%. In the theoretical part of the same paper, trajectory calculations confirmed the observed H/D isotope effect. Moreover, the theory predicted only a slight temperature dependence of the product yields of CO and CH₂O as well as a 15% CO yield for CH₃ + O. All these studies were sparked by a publication by Seakins and Leone⁴ reporting a product yield for CO of 0.4 ± 0.2 at room temperature. A large CO-producing branch could have had serious consequences for the combustion of small hydrocarbons, where this reaction is a major pathway for methyl radical consumption.

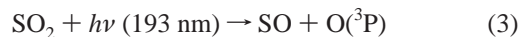
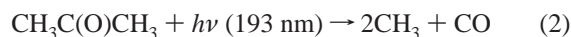
In this paper, we present the temperature dependence of the rate constant and product yield for the reaction of methyl radicals

with oxygen atoms. Using isotopic labeling of one of the reactants, we were also able to measure the CO yield for CD₃ + O.

Experimental Section

Two experimental methods have been used to study reaction 1. The temperature dependence of the reaction kinetics and product yields for the two major reaction channels (1a) and (1b) have been measured using our repetitively sampled time-of-flight mass spectrometer. Because mass spectrometry is somewhat limited with respect to identifying species of the same mass and also suffers from interferences due to fragmentation, notably CO/CH₂O, we determined the CO yield for the CD₃ + O case using tunable diode laser absorption spectroscopy. Detailed descriptions of both apparatuses have been published elsewhere and only an overview will be given below.^{1,2,5}

In both experiments, methyl radicals and ground state oxygen atoms were conveniently produced in the cophotolysis of acetone and sulfur dioxide, SO₂, at $\lambda = 193 \text{ nm}$ using a pulsed ArF-excimer laser (Lambda Physik LPX 240i or Compex 100) as the radiation source



Acetone (Mallinckrodt, 99.5%) and perdeuteroacetone (Aldrich, 99.5 D-atom %) were degassed with three freeze–pump–thaw cycles before use. Both compounds, as well as S¹⁸O₂ (Stohler, 99.5 atom %, no longer available), were stored as dilute gaseous mixtures in He or Ar (Praxair, UHP grade, 99.998%) in 20 l glass bulbs. SO₂ that was used in the TOFMS study was

* To whom correspondence should be sent. E-mail: fknberg@bnl.gov.

† E-mail: preses@bnl.gov.

purchased as a 5% mixture in He (Praxair, SO₂ ≥ 99.6%, He UHP-grade). For calibration purposes, mixtures of CO (Matheson, > 99%), C¹⁸O (Icon Services Inc., 98 atom %), and CH₂O/CD₂O with He or Ar were prepared in additional glass bulbs. Both formaldehyde isotopomers were prepared by heating the respective paraformaldehyde (Aldrich, CH₂O 95%, CD₂O 99 D-atom %) to a temperature around 100 °C. Gaseous formaldehyde was then collected in a liquid nitrogen trap, transferred to a glass bulb on warming, and diluted with He. Typically, the preparation of the gas mixtures was performed a sufficiently long time before use to ensure complete mixing.

TOFMS. The reactor consists of a tubular quartz reactor (diameter 1 cm, length 43 cm), which could be electrically heated. The surface was coated with boric acid and heat treated at 450 °C in a vacuum. This procedure greatly reduced the loss of oxygen atoms on the reactor wall at high temperatures. Precursor molecules mixed into bath gas (He: Praxair, UHP-grade) flowed at a constant velocity of 17 m/s through the tube. The gas flow through the reactor and precursor concentrations were set by mass-flow controllers (Tylan General, FC 260). The total pressure was adjusted according to temperature so that a constant bath gas density of [He] = 3.2 × 10¹⁶ cm⁻³ was maintained. A 1-mm pinhole in the wall of the reactor allowed the sampling of the gas mixture in the tube, a fraction of which was subsequently photoionized by VUV radiation emitted by a hollow cathode lamp (McPherson, Model 630). The lamp was operated with either He (*hν* = 21.2 eV) or Ar (*hν* = 11.62 and 11.83 eV) in the discharge at low pressures (*p* ≤ 1 Torr). Using Ar, we could observe methyl radicals and formaldehyde essentially free from fragmentation. Helium allows us to ionize CO (ionization potential, IE = 14.01 eV)⁶ as well. However, fragmentation of acetone and formaldehyde into mass 28 and nitrogen in the background gas were the major contributors to the signal at this mass. All these effects had to be removed by way of calibration. By rapid successive extractions of these ions into the flight tube, mass spectra for all species in the reactor could be acquired simultaneously. The time between two extraction pulses was chosen to be 48 μs. With the voltages applied to extraction and acceleration grids of the TOFMS, this time interval allowed us to cover a mass range of 1 to 150 amu without having the heaviest mass of one mass spectrum interfere with the lightest mass in the following spectrum. The observation time from the moment the excimer laser fired until the reaction was completed was typically less than 15 ms corresponding to 312 individual mass spectra. However, only 12 ms were usable because at the chosen flow velocity dilution with the fresh mixture set in after that time (see Figure 1). In separate calibration experiments, temperature profiles along the axis of the reactor tube were recorded. The maximum local deviation from the average value for the temperature was not more than 5%.

The concentration of the radical species was varied by changing either the precursor concentrations (acetone: (2–6) × 10¹² molecules cm⁻³, SO₂: (2.7–8.3) × 10¹³ molecules cm⁻³), or, to a moderate extent, the laser pulse energy between 25 and 30 mJ/cm². Under these conditions, 6% to 15% of the precursor concentrations were photolyzed depending on laser fluence and temperature. Over the investigated temperature range (345–925 K) the fraction of acetone photolyzed at constant laser fluence increased by 50% in contrast to SO₂, the photolyzed fraction of which decreased by 40%.

TDLAS. For this experiment, a tubular glass cell (diameter 4 cm, length 129.5 cm) with CaF₂ windows was filled with each of the premixed binary (acetone/Ar, S¹⁸O₂/Ar) gas mixtures

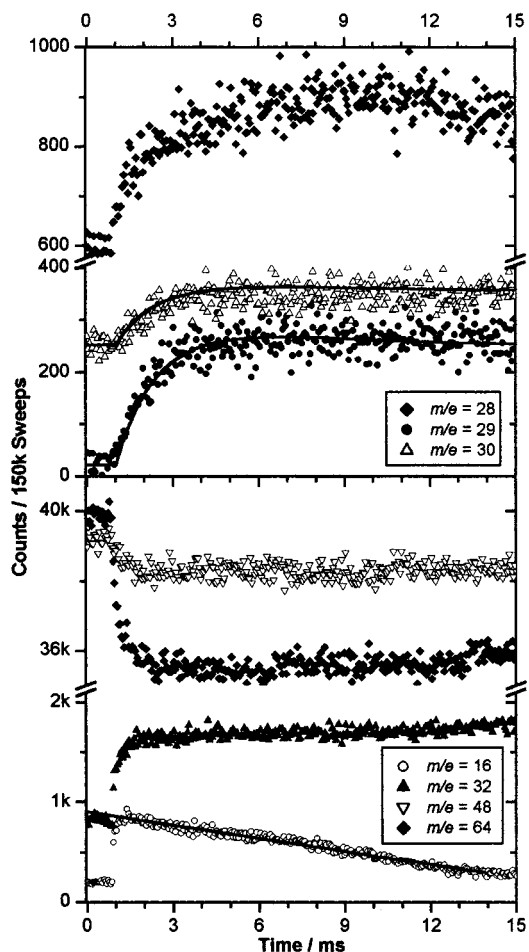


Figure 1. Ion signals plotted vs time. He-ionization, *T* = 925 K, *P* = 3.1 Torr, [Acetone] = 2.6 × 10¹² cm⁻³, [SO₂] = 3.6 × 10¹³ cm⁻³, [CH₃]₀ = 6.4 × 10¹¹ cm⁻³, [O]₀ = 4.0 × 10¹² cm⁻³. The lines in the upper panel are based on a fit to mass 29 {*k*'₁ = (688 ± 28) s⁻¹}, which was multiplied with the calibration constants for CH₂O and overlaid onto mass 30. The linear fit to mass 16 in the lower panel gives a loss constant for oxygen atoms of: *k*_{loss} = 62 s⁻¹.

to a total pressure of about 5 Torr. The experimental gas mixtures were allowed to mix for one-half hour before experiments. The unfocused excimer laser beam was used to photolyze a fraction of the precursors. Two isotopomers of carbon monoxide were produced: ¹²C¹⁸O from the reaction of ¹²CD₃ + ¹⁸O and ¹²C¹⁶O from the photolysis of acetone. We ignore products from ¹³C isotopomers. Both CO concentrations were recorded after every laser pulse from one to thirty pulses, and then after every five pulses between thirty and fifty excimer laser pulses. Three minutes were allowed after every excimer laser pulse for products to mix and thermally equilibrate. The details of the diode wavelength sweep and detection were given previously.² In brief, the diode laser was swept over a wavelength range covering the two lines with a slow (1 s) linear ramp (Figure 2). The diode wavelength was also modulated with a small amplitude sinusoidal voltage and the resulting signals were detected using a lock-in amplifier and recorded in a digital oscilloscope. This arrangement was sufficiently sensitive to detect CO concentrations from single excimer laser pulses. 256 wavelength sweeps of the diode were averaged.

The wavelength of the diode laser was calibrated using dilute mixtures of natural abundance CO in Ar and confirmed with 1:1 abundance mixtures of C¹⁶O and C¹⁸O in Ar. The ¹²C¹⁶O line used was the P(17) transition of the *v* = 0 → *v* = 1 band at 2073.265 03 cm⁻¹ and the ¹²C¹⁸O line used was the P(5)

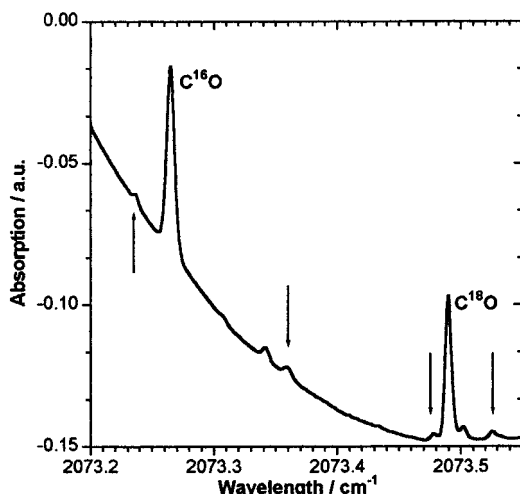


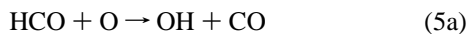
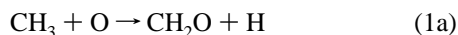
Figure 2. IR absorption spectrum after 50 excimer laser pulses. The four lines indicated by arrows are due to absorption by CD₂O product as determined by comparison with a sample of authentic CD₂O. The energies of the CD₂O absorptions are calculated to be 2073.237, 2073.360, 2073.478, and 2073.525 cm⁻¹.

transition of the $\nu = 0 \rightarrow \nu = 1$ band at 2073.489 64 cm⁻¹.⁷ Room-temperature variations were avoided because the P(17) C¹⁶O line is far from the room-temperature peak of the CO rotational distribution ($J \approx 7$), and temperature variations thus have a large effect on equilibrium rovibrational populations.

Acetone and SO₂ concentrations were chosen, based on known 193-nm absorption coefficients, 4.0×10^{-18} cm² molecule⁻¹ for acetone-*d*₆⁸ and 6×10^{-18} cm² molecule⁻¹ for S¹⁸O₂.^{9,10} and from the known CD₃ and O atom yields, so that $[O]_0/[CD_3]_0 \approx 10$.

Experimental Results

Kinetic Analysis. The temporal profiles of the concentrations of methyl radicals and formaldehyde molecules were assumed to be governed by a simple reaction mechanism



The concentrations of the precursor species (CH₃C(O)CH₃ and SO₂) were chosen so that the oxygen atom concentration was always in excess of the methyl radical concentration resulting in $[O]_0/[CH_3]_0$ ratios ranging from 7 to 15. Because reaction 1 is very fast, the fate of the methyl radicals was completely governed by reaction with oxygen atoms. Although reactions 5 and 6 have no immediate effect on the concentrations of either CH₃ or CH₂O in this mechanism, these reactions were added to simulate the profiles of all species and establish limits of validity concerning the analysis regarding the CO yield (see below). The wall loss rates of the methyl radicals in the TOFMS

experiment were determined by photolyzing acetone only and found to be less than 10 s⁻¹ at every temperature. Therefore, the wall loss rate was henceforth neglected.

To find approximate expressions for the methyl and formaldehyde concentration profiles, the oxygen atom concentration was assumed to be independent of all other species (i.e., pseudo first-order conditions). In addition, the temporal profile of the oxygen atom concentration was fit to a straight line

$$[O] = [O]_0 \times \{1 - k_{\text{loss}} \times t\}$$

Although this simplification does not capture all the details of the actual profile of the oxygen atoms, it represents the observed linear decay in all experiments adequately (see Figure 1, lower panel). The precise origin of this linear behavior is not known, but was attributed to heterogeneous reactions on the reactor wall. Numerical integration of reactions 1–8 with rate constants where they are known and reasonable assumptions where the rate constants are not known, using accurate initial species concentrations does not predict a precisely linear decay for O atoms over the observation time, but yields an initial fast decay followed by a linear decay. The amplitude of the initial fast decay is sufficiently small that the assumption of a purely linear decay does not lead to serious error. See below.

Under these assumptions, the analytical solution of the differential equation is straightforward. Although the differential equation for the methyl concentration could be integrated directly, the expression for the formaldehyde concentration was adopted from the solution to consecutive first-order reactions. The time-dependent exponential term was chosen in analogy to the solution for the methyl concentration. Differentiating this expression with respect to time leads to the desired differential equation for formaldehyde proving the validity of our *ansatz*

$$[CH_3] = [CH_3]_0 \times \exp\left(-k'_1 \times t \times \left[1 - \frac{k_{\text{loss}}}{2} \times t\right]\right)$$

$$[CH_2O] = [CH_2O]_{\text{max}} \times \left\{ \exp\left(-k'_4 \times t \times \left[1 - \frac{k_{\text{loss}}}{2} \times t\right]\right) - \exp\left(-k'_1 \times t \times \left[1 - \frac{k_{\text{loss}}}{2} \times t\right]\right) \right\}$$

with

$$[CH_2O]_{\text{max}} = [CH_3]_0 \times \frac{k_{1a}}{k_1 - k_4}$$

In these expressions $[CH_3]_0$, $[CH_2O]_{\text{max}}$, and $k'_1 (=k_1 \times [O]_0, k_1 = k_{1a} + k_{1b})$ were adjusted to fit the experimental data, whereas k_{loss} was determined directly from the oxygen atom profile. The rate of the reaction 4, $k'_4 (=k_4 \times [O]_0)$, was calculated with $k_4 = 1.77 \times 10^{-11} (T/298 \text{ K})^{0.57} \times \exp(-1390 \text{ K}/T)$ cm³ molecule⁻¹ s⁻¹.¹¹ In every signal profile, the first five mass spectra after the laser fired were neglected accommodating both the quenching of vibrationally hot methyl radicals and the time lag required for molecules to travel from the orifice in the reactor wall to the ionization region. The initial oxygen atom concentration was calculated from the drop in the SO₂ signal with a photolysis yield of one for this channel. The concentration of methyl radicals was determined from the drop in acetone. However, we used an effective yield of $\Phi_{2,\text{eff}}(\text{CH}_3) = 0.96$ for the channel giving two methyl radicals and one carbon monoxide molecule. This value is a compromise between the primary yield for CH₃ ($\Phi_2(\text{CH}_3) = 0.95$) reported by Lightfoot et al.¹² and the observations made in this laboratory, in which we confirmed

a second channel leading to ketene, CH₂CO, and methane, CH₄ ($\Phi_2(\text{CH}_2\text{CO}) \approx 0.02$).¹³ In contrast, our data indicated that the yield for a third channel giving H + CH₂C(O)CH₃ ($\Phi_2(\text{CH}_2\text{C}(\text{O})\text{CH}_3) < 0.01$) was far smaller than given by Lightfoot et al. Also, secondary photolysis of methyl radicals in the same laser pulse yields methylene radicals, CH₂, whose concentration was unfortunately below our detection limit under our experimental conditions. However, from the work of Lightfoot et al., as well as the study mentioned above, we had to assume that a small fraction (1–2%) of the methyl radicals were photolyzed. Because the methylene concentration is small compared to the concentrations of oxygen atoms or methyl radicals, this does not have a measurable effect on the kinetics.

To establish maximum error bounds, the complete mechanism as shown above was integrated numerically. Because a simple first-order loss of oxygen atoms on the reactor wall results in an exponential decay in the oxygen atom concentration, a more complex wall reaction mechanism was employed consisting of diffusion to and from the wall plus a heterogeneous reaction rate. The purpose of this approach was to attempt to duplicate the observed purely linear decay in the oxygen atom concentration. The methyl radical profiles for two scenarios were then calculated for a worst case: $[\text{O}]_0/[\text{CH}_3]_0 = 7$, and a pseudo first-order case: $[\text{O}]_0/[\text{CH}_3]_0 = 400$, which corresponds to the analytical treatment outlined above. The apparent rate constant obtained from the methyl decay for the first case was only about 10% slower than for the latter. Because this error in the reaction rate falls well into the range of uncertainty for this experiment, we chose to analyze the data according to this simplified approach.

For the case of the He discharge, fragmentation of the ionized acetone into $m/e = 15$ overwhelmed the signal of the genuine methyl radicals so that only formaldehyde was used in the kinetic analysis. At this photon energy, the fragmentation of CH₂O⁺ into HCO⁺ was the process with the highest efficiency, so that the analytical solution was fitted to the signal at $m/e = 29$. The fit was checked against the profile of the parent ion, whereby the profiles of the daughter ions were transformed according to the appropriate calibration constants resulting in profiles for the parent ion that described the actual data very well for all experiments, and thereby confirming the fit and the identity of the $m/e = 29$ channel as formaldehyde. Ionization with the Ar lamp was much more gentle leading to nearly fragmentation-free spectra, so that the signals for the parent ions of CH₃ and CH₂O were used in the fit. The resulting reaction rates, k_1 , were then plotted against the initial oxygen atom concentration. Finally, a linear fit to the data gave the rate constant for reaction 1.

With the flow velocity chosen in combination with the small diameter of the reactor tube, the overall pressure along the reactor was not constant so that corrections to the rate constants had to be made according to the pressure drop.¹⁴ Because we measured the pressure at the end of the reactor, the true pressure at the orifice was slightly higher with $\Delta P = 5.9 \times 10^{-3} \times v \times \eta \times \Delta z \times R^{-2}$, where ΔP is the pressure difference in Torr at the orifice compared to the point of measurement, v is the flow velocity in cm/s, η is the bath gas viscosity in g cm⁻¹ s⁻¹, R is the tube radius in cm, and Δz is the distance in cm of the orifice to the end of the flow tube.¹⁵ In a first-order approximation, the corrected rate constants can be given by: $k_{1,\text{corr}} = k_1 \times (1 + \Delta P/P)^{-1}$.¹⁶ This lowered all rate constants by roughly 15% where the increase in ΔP due to the temperature dependence of the viscosity was compensated by the increase in total pressure P .

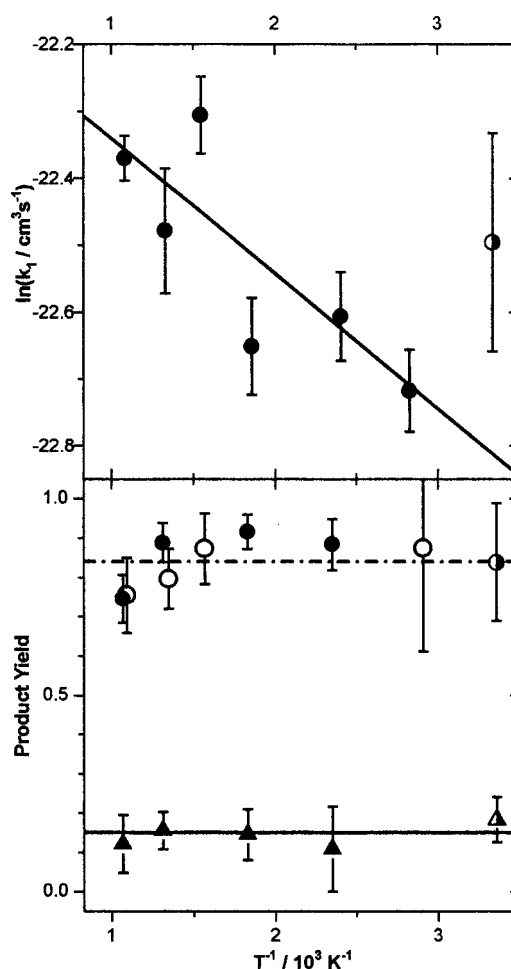


Figure 3. Upper panel: Arrhenius plot of the second-order rate constants for reaction 1. Lower panel: Plot of product yields for CH₂O and CO of reaction 1 vs inverse temperature. Average values are marked by (---) and (—), respectively. Half-filled symbols are results from an earlier measurement. Filled symbols in the lower panel are for He-discharge lamp, open symbols are for Ar.

An Arrhenius expression was then fit to the obtained corrected rate constants for reaction 1 in the temperature range of $T = 354$ to 925 K giving (errors are 2σ , see Figure 3)

$$k_{1,\text{corr}} = (2.4 \pm 0.3) \times 10^{-10} \exp(-202 \pm 60 \text{ K}/T) \text{ cm}^3 \text{ molecule}^{-1} \text{ s}^{-1}$$

It should be noted that this particular fit was done purely for convenience and is only valid in the observed temperature range, which is too narrow to describe the temperature dependence of this reaction globally. However, the important information is that the rate constant of the CH₃ + O reaction clearly shows an increase with rising temperature, contrary to previous studies, which did not detect any temperature dependence.

The rate constant for the CD₃ + O reaction was measured according to the method outlined above at a temperature of 308 K and pressure of 3 Torr (He) using H₂ in the VUV lamp. The oxygen atom concentration, however, had to be calculated this time from the increase in SO radicals because acetone-*d*₆ and SO₂ have the same mass. A similar overlap exists for CD₂O and S/O₂, whereby sulfur atoms could be either produced in the photolysis of SO₂ or originate from the fragmentation of SO ions. Therefore, only the signal from CD₃ could be analyzed. In these experiments, the concentrations of the precursor species were not changed. The excimer laser energy was adjusted

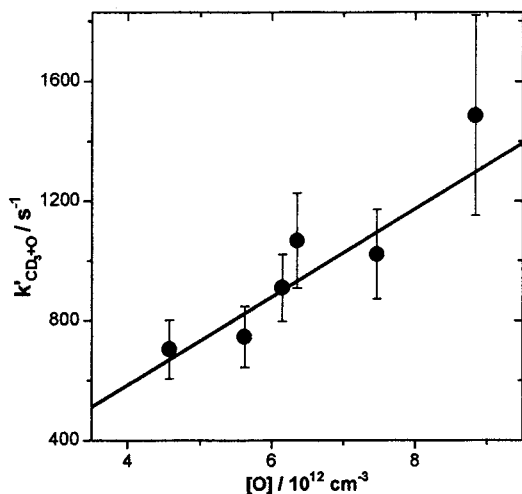


Figure 4. Second-order plot of the apparent reaction rates for $\text{CD}_3 + \text{O}$. The line is a linear fit to the data with the intercept set to zero. H_2 -ionization, $[\text{Acetone}] = 4.7 \times 10^{12} \text{ cm}^{-3}$, $[\text{SO}_2] = 3.3 \times 10^{13} \text{ cm}^{-3}$, excimer laser energy = 100–280 mJ/pulse, $[\text{O}]_0/[\text{CH}_3]_0 \approx 10$.

instead. Although this increases the likelihood of producing methylene radicals for the higher pulse energies, the influence on the CD_3 kinetics is still marginal. However, the range of the oxygen atom concentration covered was limited, which made it necessary to force the linear fit in the second-order plot through zero (see Figure 4). After pressure correction the resulting rate constant was given by: $k_{\text{CD}_3+\text{O}} = (1.3 \pm 0.8) \times 10^{-10} \text{ cm}^3 \text{ molecule}^{-1} \text{ s}^{-1}$, which is practically the same as for $\text{CH}_3 + \text{O}$. The large error given here reflects realistically all the uncertainties in this analysis.

Product Analysis (TOFMS). The yields of two products of reaction 1, CH_2O and CO , were analyzed by comparing the formaldehyde produced with the drop in acetone concentration or by comparing the two products directly. To convert counts into concentration, we simply multiplied the measured signal by the appropriate calibration constants, which were determined routinely at every temperature. This formalism has been extensively described in a previous publication.¹ In the absence of any wall loss of methyl radicals, which was generally the case, the yield of formaldehyde was given by

$$\Phi_1(\text{CH}_2\text{O}) = \frac{k_{1a}}{k_1} = \frac{[\text{CH}_2\text{O}]_{\text{corr}}/(\Delta[\text{acetone}] \times 2 \times \Phi_{2,\text{eff}}(\text{CH}_3))}{[\text{CH}_2\text{O}]_{\text{corr}}}$$

with

$$[\text{CH}_2\text{O}]_{\text{corr}} = \left(\frac{k_1 - k_4}{k_1} \right) \times [\text{CH}_2\text{O}]_{\text{max}}$$

Assuming that CO and CH_2O are the only products of reaction 1, the CO yield can then be calculated from

$$\Phi_1(\text{CO}) = \frac{k_{1b}}{k_1} = \frac{[\text{CO}]}{([\text{CO}] + [\text{CH}_2\text{O}]_{\text{corr}})}$$

This implies that the only source for carbon monoxide is reaction 1. Unfortunately, methylene radicals, although undetected, might contribute CO through the fast reaction of¹¹



Even if the yield of channel (9a) were one, this would cause an increase in the calculated CO yield by only 10%. Moreover, methylene radicals could be scavenged by SO_2 and probably SO radicals, although references to this reaction could not be found. In view of these uncertainties, we are going to present here the uncorrected values for the CO yield. In addition, HCO radicals produced in reaction 4 can lead to an additional signal at mass 28 through fragmentation after ionization or subsequent reactions with oxygen atoms (reaction 5a). Simulation calculations using the complete mechanism (see above) showed that measuring the CO concentration in a narrow interval (± 0.5 ms) around the maximum of the CH_2O profile introduces only a small error in the CO concentration ($\leq 5\%$). However, with the increased production of HCO radicals in the reaction system at $T = 925$ K, the uncertainties in the CO yield do not justify the use of this value in the further analysis.

Since no trend in the individual product yields with temperature could be detected (see Figure 3 lower panel), only averaged yields for CH_2O and CO are being reported here with $\Phi_1(\text{CH}_2\text{O}) = 0.84 \pm 0.12$ and $\Phi_1(\text{CO}) = 0.15 \pm 0.06$ for $T = 354 - 925$ K. Errors are 2σ . These results also confirm that formaldehyde and carbon monoxide are the only dominant carbon-containing products of reaction 1. In addition, these observations are in excellent agreement with theoretical calculations published by Marcy et al. who predicted a CO yield of 0.15 at room temperature, which only slightly decreases with temperature to 0.13 at 1000 K.

Product Analysis (TDLAS). Recorded signals for the two CO isotopomers were numerically integrated and converted to CO concentrations by comparison with absorptions from known $\text{C}^{16}\text{O}/\text{C}^{18}\text{O}$ mixtures acquired by the same method (see Figure 5 upper panel). Because two methyl radicals are produced for each CO in the photolysis of acetone, the product yield for this reaction is given by

$$\Phi_{\text{CD}_3+\text{O}}(\text{C}^{18}\text{O}) = [\text{C}^{18}\text{O}]/2 \times [\text{C}^{16}\text{O}]$$

Therefore, the shot-by-shot $[\text{C}^{18}\text{O}]/[\text{C}^{16}\text{O}]$ ratio was calculated, multiplied by 1/2, and the resulting points were fitted to a straight line. Extrapolating the fit to zero laser pulses then gave the final CO product yield (see Figure 5 lower panel).

Accurate measurement of the CO yield from the reaction requires that CO not be produced by “dark” reactions between reactants and/or products in the interval between laser pulses. The signature of the presence of these unwanted reactions would be an increase in the C^{18}O concentration between laser pulses on a ≥ 0.1 s time scale, which is determined mainly by the rate constant of the $\text{CD}_2\text{O} + \text{O}$ reaction (assumed to be of the same magnitude as the rate constant for $\text{CH}_2\text{O} + \text{O}$). To verify that these reactions did not interfere, the diode laser frequency was locked (in separate experiments) to each of the CO wavelengths used and the concentration of CO was followed in real time (using lock-in detection in second-harmonic with a 1 ms time constant) after single excimer laser pulses. Pressures used were similar to those during the yield experiments. Upon irradiation by the excimer laser, both CO signals rose on a millisecond time scale, i.e., the $\text{CD}_3 + \text{O}$ kinetics could not be temporally resolved due to limitations set by the lock-in. After mixing was complete (~ 0.01 s), neither isotopomer showed any growth in its concentration indicating that dark reactions were not significant under our reaction conditions. Only the accumulation of reaction products and subsequent reactions (most probably initiated by $\text{CD}_2\text{O} + \text{O} \rightarrow \text{DCO} + \text{OD}$) gave rise to a small increase in the $[\text{CO}]$ -ratio with the number of excimer laser

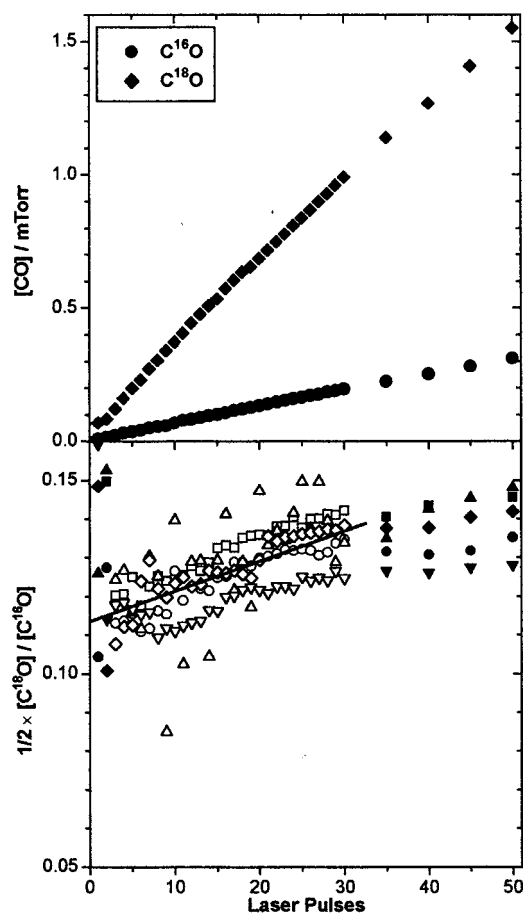


Figure 5. Upper panel: Absolute CO concentration vs laser pulses for a single experiment. Lower panel: C¹⁸O product yield vs excimer laser pulses for five separate experiments. The line is a linear fit to all data points shown as open circles. Points not fit include very low CO concentrations where the value of the CO concentration was comparable to the uncertainty in the measurement and high CO concentrations where the influence of secondary chemistry begins to distort the CO concentrations.

pulses. The extrapolation of the CO yield to zero laser pulses avoids any interference from this source.

Generally, the same considerations regarding secondary photolysis of methyl radicals have to be made also for this experiment. Fortunately, the photon density was even less than in the TOFMS measurements (≤ 20 mJ/cm²) so that the methylene chemistry can be safely neglected. However, at room temperature and a pressure of 5 Torr, CD₃ recombination reactions cannot be ruled out. Assuming a rate constant for the recombination being the same as for CH₃ ($k_{\infty} = 6 \times 10^{-11}$ cm³s⁻¹),¹⁷ only 96% of the deuterated methyl radicals react with oxygen atoms. Therefore, the observed yield must be multiplied by a factor of 1.04 to account for the missing methyl radicals. With the extrapolated value for the yield of 0.114 this gives a corrected yield of $\Phi_{\text{CD}_3+\text{O}}(\text{C}^{18}\text{O}) = 0.12 \pm 0.01$ (2σ). Thus, replacing CH₃ with CD₃ reduces the CO yield by a factor of 2/3 compared to the CO yield for the CH₃ + O reaction ($\Phi_{\text{CH}_3+\text{O}}(\text{CO}) = 0.18 \pm 0.04$).²

Discussion

Regarding the absolute CO yield of reaction 1 and its isotope effect, the agreement among the experimental and theoretical studies by Marcy et al.³ and the present and previous work^{1,2} in our group is remarkable. In addition, one of the assumptions made in the analysis of the experiments of Marcy et al., that is,

no significant differences between the rate constants of the CH₃ + O and CD₃ + O reactions, was verified here. However, the predicted 13% decrease in the CO yield with temperature could not be detected. This might be a consequence of the scatter in our experimental data, which were not precise enough to observe these small changes.

The accepted mechanism for this reaction involves the initial formation of a highly energized methoxy complex, CH₃O*, that undergoes direct dissociation or, presumably, isomerization to CH₂OH followed by dissociation into products. The main dissociation channel leads to a simple elimination of a hydrogen atom from the complex giving H + CH₂O with a transition state about 240 kJ/mol below the energy level of the entrance channel. The only exothermic channel producing CO also leads to H₂ as coproduct. However, electronic structure calculations^{3,18} did not produce any stationary points on the potential surface that could explain a direct H₂ loss from the methoxy complex. Two indirect channels, CH₂O → H₂ + CO and CH₂OH → H₂ + COH, are either energetically inaccessible or unfavorable compared to the simple hydrogen loss from CH₃O* and, therefore, could not give a CO yield as high as observed. Interestingly, in their trajectory calculations Marcy et al. found that the energy released in the initial addition of a methyl radical to an oxygen atom was sufficient for the reaction to proceed directly over the barrier separating CH₃O from H₂ + HCO, where the top of the barrier still is about 120 kJ/mol below the CH₃ + O energy level. Thus, this channel does not proceed over a transition state at all and conventional transition state theory cannot be applied in this case to explain the product distribution. Other trajectories started out in the direction of a simple hydrogen loss but were diverted toward the transition state belonging to a hydrogen abstraction from formaldehyde: H•••HCHO. This process, called frustrated hydrogen loss, was attributed to a large orbital barrier prohibiting the hydrogen atom from leaving the complex. This dynamic effect is smaller for heavier atoms, hence the CO yield for the reaction of CD₃ + O is smaller. For low angular momenta frustrated hydrogen loss was as important as the direct crossing of the barrier in producing CO. However, direct crossing was the dominant pathway at high *J* values.

With respect to the rate constant of reaction 1, the agreement with literature data is not as good. In the most recent experimental studies on the temperature dependence of the rate constant, Slagle et al. (300–900 K)¹⁹ and Lim and Michael (1610–2000 K)²⁰ measured a temperature independent rate constant of $k_1 = 1.4 \times 10^{-10}$ cm³ molecule⁻¹ s⁻¹. Moreover, in additional theoretical calculations on the rate of reaction 1 continuing the work of Marcy et al., Harding confirmed the results of Slagle and Lim.²¹ In light of these findings, the temperature dependence of k_1 found here has to be reconsidered carefully. Possible errors include an increased loss of methyl radicals due to wall reactions, which, however, were measured to be negligible at all temperatures. Reactions of methyl radicals with species other than oxygen atoms would have altered the product yields for CH₂O and CO considerably, which was not detected either. Systematic errors in the gas flow and the pressure in the reactor leading to higher precursor concentrations with increasing temperatures could be ruled out as well. The consequence of such an error would have been larger calibration constants, which, however, did not change in the observed temperature range. Although the clustering of faster reaction rates on the high-temperature side is indicative of the existence of a temperature dependence, it has to be noted that the rate constant could also be given by an average value of $(1.7 \pm 0.5) \times 10^{-10}$

$\text{cm}^3 \text{ molecule}^{-1} \text{ s}^{-1}$, whereby the 2σ error encompasses all measured rate constants. This value would then be in good agreement with literature data.¹¹ Assuming k_1 to be temperature independent is probably a good choice especially for the temperatures encountered in combustion systems.

Summary

We have measured the kinetics and product distributions for the $\text{CH}_3 + \text{O}(^3\text{P})$ reaction between room temperature and 925 K using time-of-flight mass spectrometry. The yields for the dominant products CH_2O and CO were found to be independent of temperature, but the rate constant increased slightly with temperature. We used tunable diode laser spectroscopy to determine the CO yield from $\text{CD}_3 + \text{O}$ at room temperature. The measured yields from both experimental techniques were in excellent agreement with theoretical prediction.

Acknowledgment. This work was performed at Brookhaven National Laboratory under Contract DE-AC02-98CH10886 with the U.S. Department of Energy and supported by its Division of Chemical Sciences, Office of Basic Energy Sciences.

References and Notes

- (1) Fockenberg, C.; Hall, G. E.; Preses, J. M.; Sears, T. J.; Muckerman, J. T. *J. Phys. Chem. A* **1999**, *103*, 5722.
- (2) Preses, J. M.; Fockenberg, C.; Flynn, G. W. *J. Phys. Chem. A* **2000**, *104*, 6758.
- (3) Marcy, T. P.; Díaz, R. R.; Heard, D.; Leone, S. R.; Harding, L. B.; Klippenstein, S. J. *J. Phys. Chem. A* **2001**, *105*, 8361.
- (4) Seakins, P. W.; Leone, S. R. *J. Phys. Chem.* **1992**, *96*, 4478.
- (5) Fockenberg, C.; Bernstein, H. J.; Hall, G. E.; Muckerman, J. T.; Preses, J. M.; Sears, T. J.; Weston, R. E., Jr. *Rev. Sci. Instr.* **1999**, *70*, 3259.
- (6) Erman, P.; Karawajczyk, A.; Rachlew-Kallne, E.; Stromholm, C.; Larsson, J.; Persson, A.; Zerne, R. *Chem. Phys. Lett.* **1993**, *215*, 173.
- (7) Guelachvili, G.; Rao, K. N. *Handbook of Infrared Standards*; Academic Press: Orlando, FL, 1986.
- (8) Rudolph, R. N.; Hall, G. E.; Sears, T. J. *J. Chem. Phys.* **1996**, *105*, 7889.
- (9) Golomb, D.; Watanabe, K.; Marmo, F. F. *J. Chem. Phys.* **1962**, *36*, 958.
- (10) Manatt, S. L.; Lane, A. L. *J. Quant. Spectrosc. Radiat. Trans.* **1993**, *50*, 267.
- (11) Baulch, D. L.; Cobos, C. J.; Cox, R. A.; Esser, C.; Frank, P.; Just, T.; Kerr, J. A.; Pilling, M. J.; Troe, J.; Walker, R. W.; Warnatz, J. *J. Phys. Chem. Ref. Data* **1992**, *21*, 411.
- (12) Lightfoot, P. D.; Kirwan, S. P.; Pilling, M. J. *J. Phys. Chem.* **1988**, *92*, 4938.
- (13) Wang, B.; Fockenberg, C. *J. Phys. Chem. A* **2001**, *105*, 8449.
- (14) Kaufmann, F. Reactions of Oxygen Atoms. In *Progress in Reaction Kinetics*; Porter, G., Ed.; Pergamon Press: Oxford, 1961; Vol. 1; p 1.
- (15) Howard, C. *J. Phys. Chem.* **1979**, *83*, 3.
- (16) Oser, H.; Walter, D.; Stothard, N. D.; Grotheer, O.; Grotheer, H. H. *Chem. Phys. Lett.* **1991**, *181*, 521.
- (17) Hessler, J., P.; Ogren, P. J. *J. Phys. Chem. A* **1996**, *100*, 984.
- (18) Walch, S. P. *J. Chem. Phys.* **1993**, *98*, 3076.
- (19) Slagle, I. R.; Sarzynski, D.; Gutman, D. *J. Phys. Chem.* **1987**, *91*, 4375.
- (20) Lim, K. P.; Michael, J. V. *J. Chem. Phys.* **1993**, *98*, 3919.
- (21) Harding, L. B., personal communication.